AD_____
_____

Award Number:
W81XWH-12-1-0025

TITLE:
Advanced Imaging Approaches to Characterize Stromal and Metabolic Changes in in Vivo Mammary Tumor Models

PRINCIPAL INVESTIGATOR:
Pamela A. Young

CONTRACTING ORGANIZATION: University of Wisconsin System, Madison, WI 53715

REPORT DATE:
March 2014

TYPE OF REPORT:
Annual Summary

PREPARED FOR: U.S. Army Medical Research and Materiel Command
Fort Detrick, Maryland 21702-5012

REPORT DOCUMENTATION PAGE

Form Approved
OMB No. 0704-0188

1. REPORT DATE	2. REPORT TYPE	3. DATES COVERED
March 2014	Annual Summary	1 Mar 2013 - 28 Feb 2014

4. TITLE AND SUBTITLE

Advanced Imaging Approaches to Characterize Stromal and Metabolic Changes in In Vivo Mammary Tumor Models

5a. CONTRACT NUMBER

5b. GRANT NUMBER W81XWH-12-1-0025

5c. PROGRAM ELEMENT NUMBER

6. AUTHOR(S)

Pamela A. Young

E-Mail: payoung2@wisc.edu

5d. PROJECT NUMBER

5e. TASK NUMBER

5f. WORK UNIT NUMBER

7. PERFORMING ORGANIZATION NAME(S) AND ADDRESS(ES)

UNIVERSITY OF WISCONSIN SYSTEM
21 N PARK ST ST E 6401
MADISON WI 53715-1218

8. PERFORMING ORGANIZATION REPORT NUMBER

9. SPONSORING / MONITORING AGENCY NAME(S) AND ADDRESS(ES)

U.S. Army Medical Research and Materiel Command
Fort Detrick, Maryland 21702-5012

10. SPONSOR/MONITOR'S ACRONYM(S)

11. SPONSOR/MONITOR'S REPORT NUMBER(S)

12. DISTRIBUTION / AVAILABILITY STATEMENT

Approved for Public Release; Distribution Unlimited

13. SUPPLEMENTARY NOTES

14. ABSTRACT

My goal is to investigate the connection between cancer cell progression and the cellular microenvironment, specifically by examining the effects of collagen density on cellular metabolism in breast cancer cells. Normal (MCF10A) and invasive (MCF10-Ca1d) breast epithelia cells were cultured in 2D and analyzed using high resolution to examine intracellular effects from cellular stress. To stress cellular metabolism, the cells were treated with either 1% O2 or DFOM, to mimic a hypoxic response, or 2DG to induce a hypoglycemic environment. Fluorescence lifetime data were then collected for the NAD(P)H and FAD within the cells. DFOM, 1%O2, and 2DG treatment caused a decrease in the free fraction of NAD(P)H and in lactate production, indicating the hypoxia response in MCF10a and MCF10-Ca1d cells may not be as simple as an increase in glycolysis. Utilizing the mammary imaging window technique in GFP-CFMS transgenic mouse, tumor cells decrease in the free fraction of NAD(P)H compared to other cells types in and around the tumor. We did not see significant changes in fluorescence lifetime of NAD(P)H between the PyVT/Col1a1 mice and PyVT/wild-type mice.

15. SUBJECT TERMS

Multiphoton Fluorescence Excitation Microscopy, Fluorescence Lifetime Imaging Microscopy, Extracellular Matrix, Mammary Imaging Window

16. SECURITY CLASSIFICATION OF:			17. LIMITATION OF ABSTRACT	18. NUMBER OF PAGES	19a. NAME OF RESPONSIBLE PERSON
a. REPORT	b. ABSTRACT	c. THIS PAGE			USAMRMC
U	U	U	UU	16	19b. TELEPHONE NUMBER *(include area code)*

Table of Contents

Introduction:

Increased mammographic density is linked to a four to six-fold increased risk of breast carcinoma (*1*). Importantly, increased breast density is associated with not only increased cellularity, but also with a significant increase in the deposition of extracellular matrix (ECM) components, especially collagen. Increased deposition of collagen and other ECM proteins surrounding tumors, termed desmoplasia, is associated with poor prognosis. The molecular basis for the effects of dense breast tissue on development of breast carcinoma is not fully understood, however we have found that increased collagen density results in a three-fold increase in mammary tumor formation, invasion, and metastasis in a dense collagen mouse model (*2*). Our lab has also shown that the structure and alignment of collagen is highly related to cancer invasion and progression (*3*). Specific Tumor-Associated Collagen Signatures (TACS) were identified that manifest in specific ways during tumor progression and that correspond to patient outcome (*4*). Additionally, we have demonstrated that changes in local collagen density can promote adhesive signaling, and enhance cell proliferation and cell migration in vitro. An increase in local collagen deposition is particularly relevant, as tumor cells migrate through and along aligned tracks of collagen fibers (*3, 5*). Thus, changes in the local deposition of collagen surrounding tumors are likely to promote tumor cell invasion.

In addition to the stromal environment, there is compelling data demonstrating metabolic changes in carcinoma cells (*6*). We previously observed changes in metabolic co-factors in mouse biopsies (*2*), cell culture (*7*), and pathology slides (*8*). While these were *ex vivo* observations, they provided a compelling snapshot of what might be occurring. A complete understanding of how cancer cells interact with normal tissue environments requires the ability to observe the relationship between subcellular structures, the microenvironment of the tumor, and components of the ECM intravitally within a 3D environment.

Multiphoton fluorescence excitation microscopy (MPM) is a laser-scanning microscopy technique that uses nonlinear excitation to non-invasively image a narrowly defined optical plane deep within tissues with spatial resolution of less than a micron. MPM is particularly well-suited for intravital studies of tumor biology in animal models because of the large depth of field and endogenous fluorescence. The intrinsically fluorescent metabolic co-factors, NADH and FAD, have been used to calculate the redox ratio, providing useful insight into cellular metabolism (*9*) and demonstrate differences between metabolic signatures of tumor and normal tissue. Additionally, MPM systems are capable of collecting second harmonic generation (SHG) signals which are a nonlinear optical property of collagen. Observations of living cells or tissues through nonlinear optical microscopy can thus provide insights into dynamic behavior, such as the progression of TACS that cannot be obtained from observations of fixed specimens.

Our preliminary data suggests a relationship between cellular metabolic changes and TACS. So we proposed a series or advanced imaging experiments to examine the interplay of cellular metabolism and collagen at the cellular level. During Year 1 of this fellowship, I focused on the characterization of endogenous optical biomarkers as a measure of cellular metabolism in vitro under known hypoxic and hypoglycemic stressors by measuring changes of the fluorescence lifetime of NADH in two-dimensional (2D) and three-dimensional (3D) cell culture. Although in

2D, there was not a statistically significant change in the lifetime of DFOM or 2DG treated MCF10A or MCF10-Ca1d cells, there was a trend demonstrating that 2DG treatment reduced the free fraction of NADH to the same level as the MCF10a cells. In 3D, increasing collagen density caused a decrease in fluorescence lifetime and an increase in the free fraction of NADH for nearly all cell type and treatment conditions. In most cases DFOM treatment or 2DG treatment caused a decrease in the free fraction of NADH, but for the MCF10-Ca1d cells in high density, DFOM treatment caused an increase in the free fraction of NADH and for the MCF10A cells in high density, 2DG caused an increase in the free fraction of NADH.

Body:

During Year 2, I went on to further investigate the effects of hypoxia and hypoglycemia on MCF10A or MCF10-Ca1d cells by using higher resolution to examine intercellular effects and by comparing the effects of a hypoxia chamber to induce hypoxic stress to DFOM treatment. I began by trying to understand the result from year 1 showing a decrease in free NADH in MCF10a and MCF10-Ca1d cells treated with DFOM. I would expect DFOM and 2DG to have opposite effects on the free to bound ratio of NADH because DFOM inhibits oxidative phosphorylation and 2DG inhibits glycolysis. However, I saw that both treatments caused a decrease in the free fraction of NADH. Therefore I did a lactate assay on media from the MCF10a and MCF10-Ca1d cells with DFOM or 2DG treatment to ascertain how glycolytic the cells are. Because lactate is an end product of glycolysis in the absence of oxidative phosphorylation, I would expect 2DG to cause a decrease in lactate due to the decrease in glycolysis, and I would expect an increase in lactate with DFOM treatment which should only inhibit oxidative phosphorylation and not glycolysis. However in both the MCF10a and MCF10-Ca1d cells, I saw a decrease in lactate with both the DFOM treatment and the 2DG treatment. This is in good agreement with the trends I saw with the FLIM data, and demonstrates that the metabolic state of these cells cannot be simplified to glycolytic vs. oxidative.

I then went on to investigate the fluorescent lifetime of NADH and FAD using higher resolution to attempt to tease apart the details that may be used intravitally to distinguish metabolic states of the cells. We saw with low resolution that MCF10-Ca1d cells have a greater free fraction of NADH than MCF10a cells. But 2DG treatment brings the free fraction of NADH to similar levels to the MCF10a cells. Using higher resolution revealed that 2DG treatment of both MCF10a and MCF10-Ca1d caused an increase in orange punctate areas within the cell. We suspect these punctate areas are mitochondria and the increase in bound NADH is associated with an increase in mitochondrial metabolism mechanisms like oxidative phosphorylation due to 2DG treatment inhibiting glycolysis in the cytoplasm.

We also looked at free FAD and found the MCF10-Ca1d cells have more blue punctate areas than the MCF10a cells indicating an increase in the free fraction of FAD. And 2DG treatment of MCF10-Ca1d cells caused an increase in the free fraction of FAD as indicated by an increase in blue punctate areas. 2DG treatment did not seem to have a large effect on the MCF10a cell morphology when we used high resolution.

I then went on to use higher resolution to compare 100uM DFOM treatment for 24 hours to 1% O2 for 24 hours using a hypoxia chamber. I found both DFOM treatment and hypoxia treatment

caused a decrease in the free fraction of NADH for MCF10a and MCF10-Ca1d cells. In both MCF10a and MCF10-Ca1d cells there appears to be an increase in the orange punctate structures similar to 2DG treatment. However the cytosol seems to become less blue and more green in many of the MCF10a cells with DFOM/hypoxia treatment consistent with a decrease in the free fraction of NADH in the cytosol, while 2DG treatment did not seem to affect the cytosol of the MCF10a cells. However the reverse seems to be the case for the MCF10-Ca1d cells. The DFOM/hypoxia treatment did not seem to affect the free fraction of NADH in the cytosol, but the 2DG treatment seemed to cause a decrease in the free fraction of NADH in the cytosol. Further quantification is necessary to confirm this and use of a mitochondrial marker to separate cytosol from mitochondria would be extremely useful.

Additionally Year 2 was spent optimizing the mammary imaging window technique for FLIM, so I can apply these insights to tumor tissue in vivo. Collaboration with Dave Entenberg from the Albert Einstein Institute brought us a new window design that reduces movement artifact so well, we are able to collect the 120 second acquisitions necessary to acquire enough photon counts for good bi-exponential fitting. This new fixturing uses at metal ring with a groove for the skin and a purse string suture to pull the skin into the groove, keeping the window in place. The metal ring then locks into the microscope stage for extreme stability.

Extremely stable intravital images can then be collected with nearly no breathing artifact. Fluorescent labeling is not required to get good contrast of tumor tissue which can be easily distinguished by morphology using endogenous fluorescence and SHG. The tumor is very bright in the NAD(P)H channel, but dim in the FAD and SHG channel. There are FAD bright cells in the stroma which we hope to characterize using fluorescent lifetime.

To this effect, we acquired a GFP-CFMS transgenic mouse that expresses GFP in the monocyte lineage cells. We collected NAD(P)H FLIM and used the GFP channel to mask out the GFP-expressing cells. We then used a region of interest based on morphology to define the tumor and compare the fluorescent lifetime of NAD(P)H in these two regions. We found a significant decrease in tau mean in the GFP-expressing cells. This is associated with an increase in free fraction of NAD(P)H. We repeated this experiment with a mouse that was not expressing GFP and used the FAD channel to mask the FAD bright cells similar to our analysis with the GFP cells in the GFP mouse, and we found the same shift in NAD(P)H lifetime seen with the GFP mice. This leads us to hypothesis that the FAD bright cells may be from the monocyte lineage. However, much more characterization is necessary.

We went on to compare the NAD(P)H fluorescence lifetime of tumor cells and FAD bright cells in the PyVT-Col1a1 model. However we did not see significant changes in fluorescence lifetime between the PyVT/Col1a1 mice and PyVT/wild-type mice in either the tumor or the FAD bright population. There was a possible trend for an increase in tau mean (corresponding to a decrease on the free fraction of NAD(P)H) which contradicts the work done in 3D culture in collagen gels that showed a decrease in tau mean with increase collagen density. Because tissue is heterogeneous, this trend may have been from a difference in local collagen structure. Analysis techniques for the SHG channel are being developed that may lend insight into the

local collagen structure. Also, there was no statistical significance, so we need to repeat this study to improve statistics.

Key Research Accomplishments:

- Analyzed endogenous biomarkers as a measure of cellular metabolism.
- Optimized Rodent Mammary Imaging Window Technique for long-term, stable FLIM imaging of mice.
- Compared optical biomarkers cellular in tumor and stromal cells and transgenic mouse models.

Reportable Outcomes:

Young, P.A., Keely, P.J., Eliceiri, K.W. *Multiparameter Optical Imaging of the Breast Tumor Microenvironment*. Focus on Microscopy 2014, Sydney, NSW, Australia, April 13-16, 2014.

Young, P.A., Inman, D.R., Szulczewski, J.M., Elicieir, K.W., Keely, P.J. *Advances in Rodent Mammary Imaging Window Designs*. 23rd Australian Conference on Microscopy and Microanalysis 2014, Adelaide, SA, Australia, February 2-6, 2014.

Young, P.A., Grislis, A, Barber, P.R., Keely, P.J., Eliceiri, K.W. *Data Processing for Time-Domain Fluorescence Lifetime Imaging Microscopy*, in Proceedings of Microscopy and Microanalysis 2013, Indianapolis, IN, USA, August 4-8, 2013.

D Inman, PA Young, J Szulczewski, PJ Keely, KW Eliceiri. *Novel Intravital Imaging Approaches to Characterize Collagen Alignment in Defined Mammary Tumor Models*. Microscopy and Microanalysis 2013. (in preparation)

Conclusion:

In conclusion, fluorescence lifetime imaging can be used to measure changes in cellular metabolism. We found an increase in the free fraction of NAD(P)H for MCF10-Ca1d (metastatic breast cancer cells) compared to MCF10a (normal breast epithelial cells) supporting the theory that an increase in the free fraction of NAD(P)H correlates with an increase in glycolysis. However, DFOM treatment, hypoxia chamber, and 2DG treatment all caused a decrease in the free fraction of NAD(P)H as well as a decrease in lactate production indicating the hypoxia response in MCF10a and MCF10-Ca1d cells may not be as simple as an increase in glycolysis.

We also showed that our improved fixturing enables us to collect extremely stable images such that we can collect FLIM images for 120seconds. Cells in the tumor have an increase in fluorescence lifetime correlating with a decrease in the free fraction of NAD(P)H compared to other cells types separated using either GFP expression or FAD intensity to mask these cells. Further study is intended within the lab to define each cell type and its FLIM profile.

Comparison of the PyVT/Col1a1 +/- and -/- mice showed the trend of an increase in lifetime of NAD(P)H of the heterogeneous mice compare to wildtype, but there was no significant difference between mice. Further study is intended in the lab to improve statistics.

References:

1. N. F. Boyd, L. J. Martin, J. Stone, C. Greenberg, S. Minkin, M. J. Yaffe, Mammographic densities as a marker of human breast cancer risk and their use in chemoprevention. *Curr Oncol Rep* **3**, 314-321 (2001).
2. P. P. Provenzano, D. R. Inman, K. W. Eliceiri, J. G. Knittel, L. Yan, C. T. Rueden, J. G. White, P. J. Keely, Collagen density promotes mammary tumor initiation and progression. *BMC Med* **6**, 11 (2008).
3. P. P. Provenzano, K. W. Eliceiri, J. M. Campbell, D. R. Inman, J. G. White, P. J. Keely, Collagen reorganization at the tumor-stromal interface facilitates local invasion. *BMC Med* **4**, 38 (2006).
4. M. W. Conklin, J. C. Eickhoff, K. M. Riching, C. A. Pehlke, K. W. Eliceiri, P. P. Provenzano, A. Friedl, P. J. Keely, Aligned collagen is a prognostic signature for survival in human breast carcinoma. *Am J Pathol* **178**, 1221-1232 (2011).
5. P. P. Provenzano, D. R. Inman, K. W. Eliceiri, S. M. Trier, P. J. Keely, Contact guidance mediated three-dimensional cell migration is regulated by Rho/ROCK-dependent matrix reorganization. *Biophys J* **95**, 5374-5384 (2008).
6. O. Warburg, On the origin of cancer cells. *Science* **123**, 309-314 (1956).
7. D. K. Bird, L. Yan, K. M. Vrotsos, K. W. Eliceiri, E. M. Vaughan, P. J. Keely, J. G. White, N. Ramanujam, Metabolic mapping of MCF10A human breast cells via multiphoton fluorescence lifetime imaging of the coenzyme NADH. *Cancer Res* **65**, 8766-8773 (2005).
8. M. W. Conklin, P. P. Provenzano, K. W. Eliceiri, R. Sullivan, P. J. Keely, Fluorescence lifetime imaging of endogenous fluorophores in histopathology sections reveals differences between normal and tumor epithelium in carcinoma in situ of the breast. *Cell Biochem Biophys* **53**, 145-157 (2009).
9. M. C. Skala, K. M. Riching, A. Gendron-Fitzpatrick, J. Eickhoff, K. W. Eliceiri, J. G. White, N. Ramanujam, In vivo multiphoton microscopy of NADH and FAD redox states, fluorescence lifetimes, and cellular morphology in precancerous epithelia. *Proc Natl Acad Sci U S A* **104**, 19494-19499 (2007).

Supporting Data:

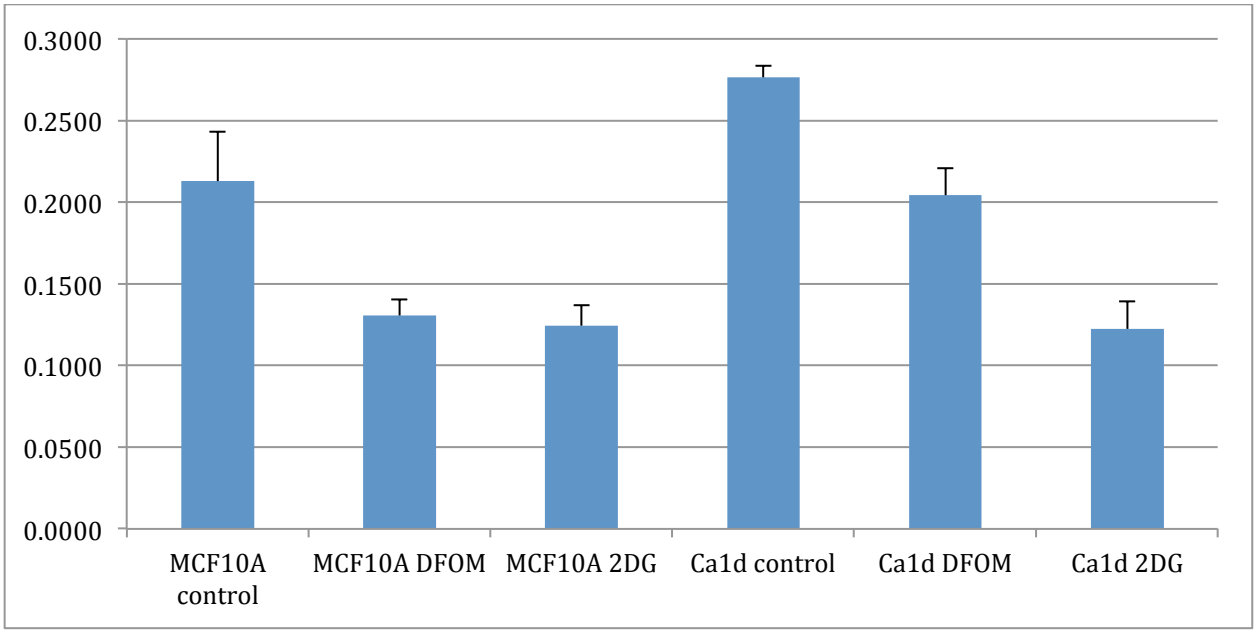

Figure 1: MCF10a and MCF10-Ca1d cells were treated with 100uM DFOM or 10mM 2DG for 24 hours then the media was collected and an Abcam colorometric lactate assay was performed and measured in arbitrary units. (N=1)

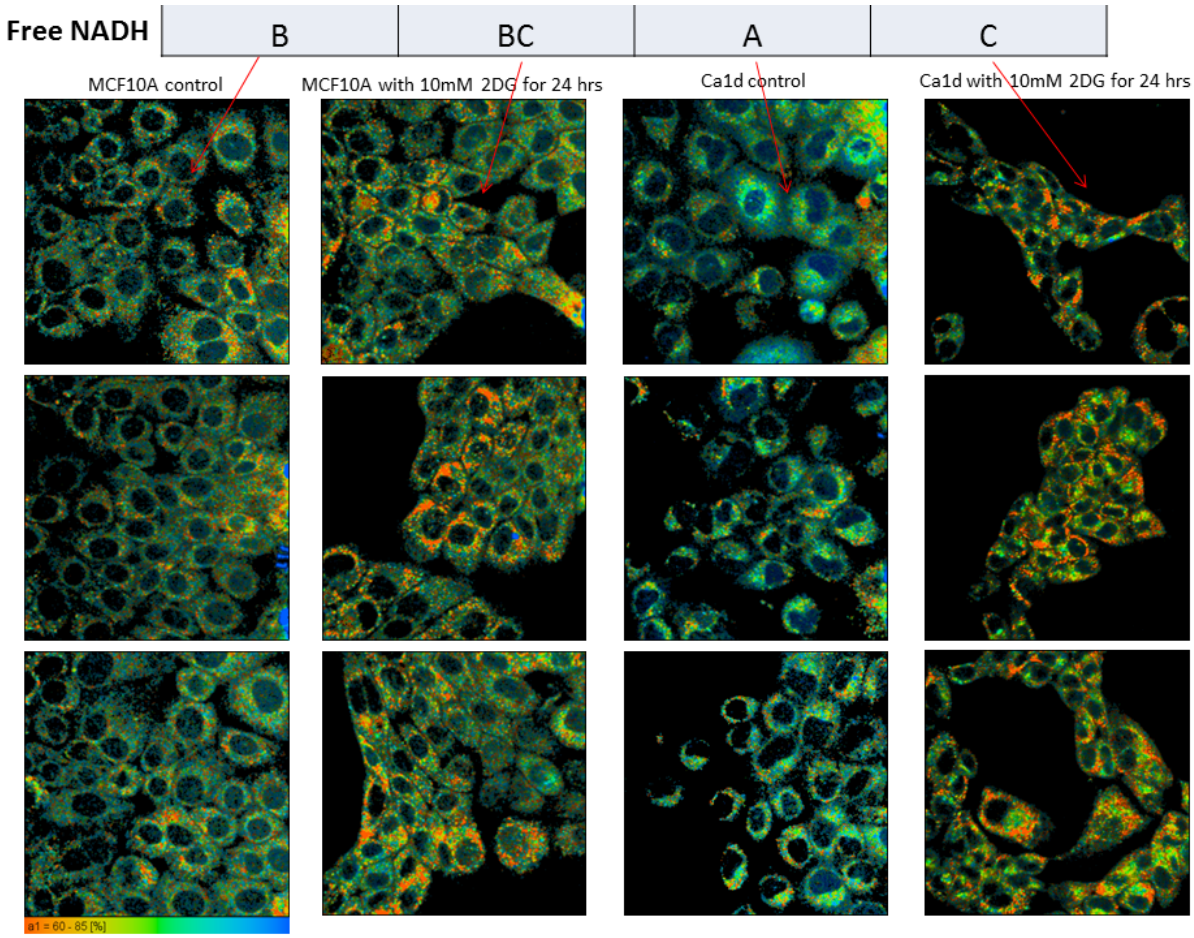

Figure 2: MCF10a and MCF10-Ca1d cells were treated with 10mM 2DG for 24 hours, and FLIM images were collected of NAD(P)H by exciting fluorescence using 780nm and collecting fluorescence using a 40x W NA 1.25 (0.7475 pix/um) and 457/50 bandpass filter. Color mapping is based on free fraction of NAD(P)H from 60% (red) to 85% (blue). Statistical significance was calculated using the 20xAir data previously reported and is reminded here using the lettering at the top.

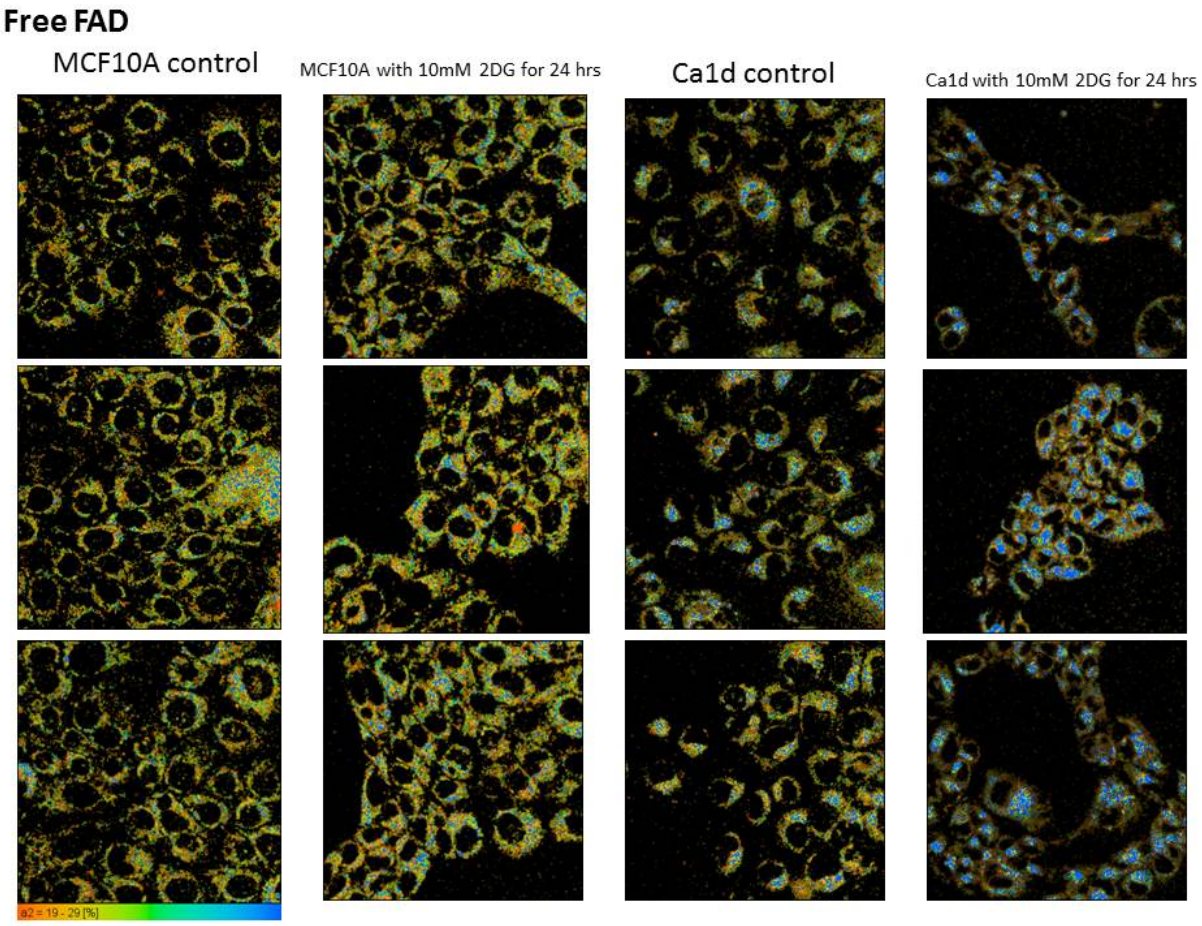

Figure 3: MCF10a and MCF10-Ca1d cells were treated with 10mM 2DG for 24 hours, and FLIM images were collected of FAD by exciting fluorescence using 890nm and collecting fluorescence using a 40x W NA 1.25 (0.7475 pix/um) and 562/40 bandpass filter. Color mapping is based on free fraction of FAD from 19% (red) to 29% (blue).

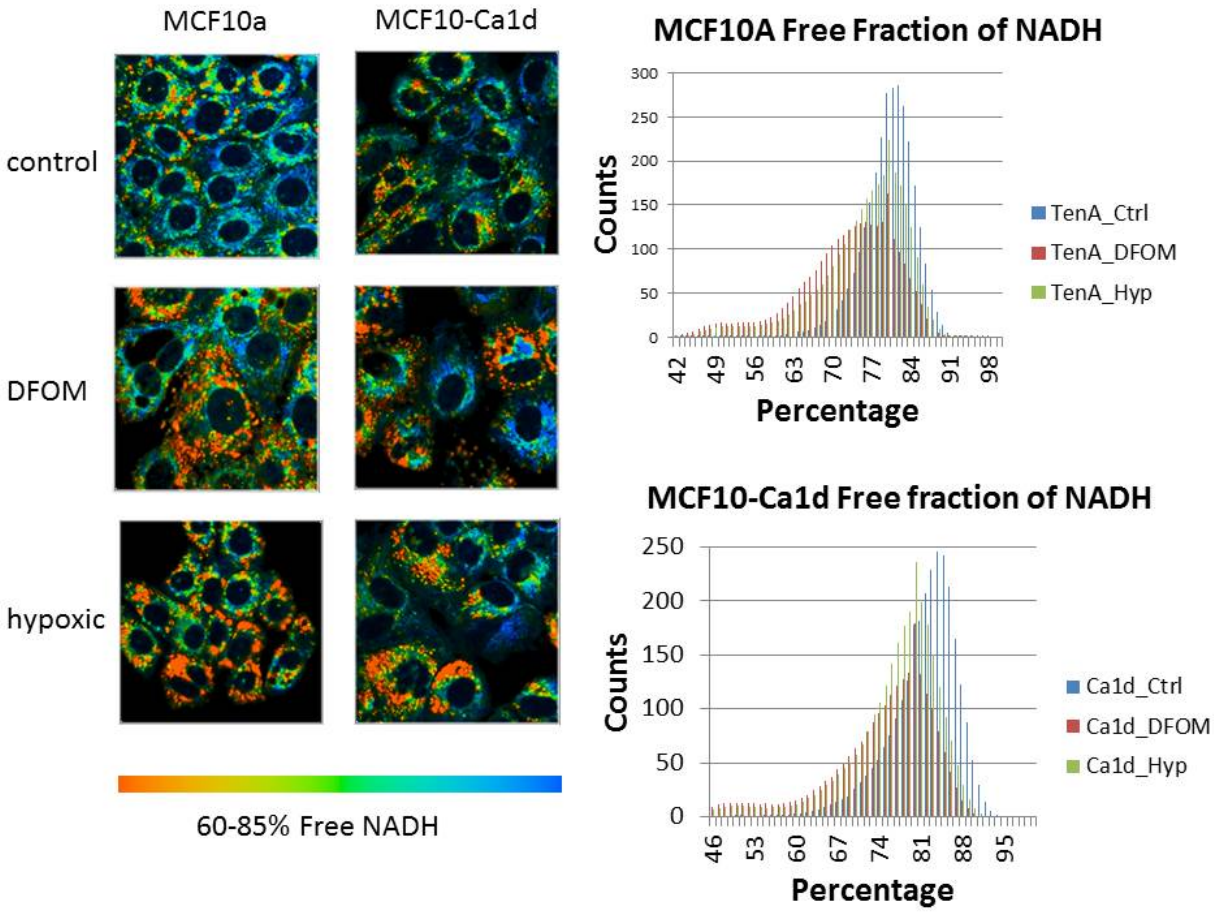

Figure 4: Comparison of 100uM DFOM treatment (21% O2, 5% CO2, N2 bal) to hypoxia chamber (1% O2, 5% CO2, N2 Bal) for 24 hours. FLIM images were excited with 740nm and collected with 60x Oil NA 1.4 (2.22 pix/um) using at 450/70 bandpass filter. Histograms are the integrated pixel counts for the free fraction of NAD(P)H from 5 images per dish. The experiment was repeated 3 times on different days.

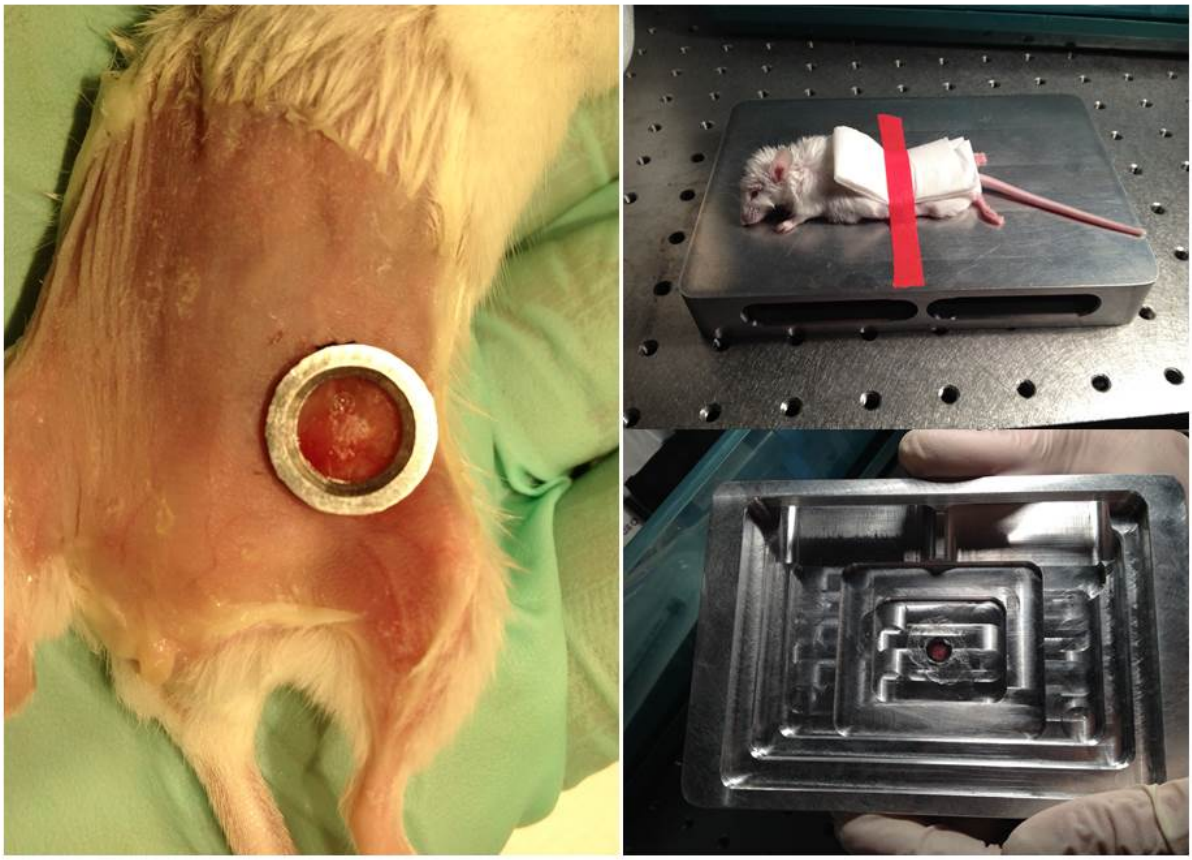

Figure 5: New fixturing for intravital FLIM imaging through a rodent mammary imaging window. Stage is raised to accommodate tall 20xW objective.

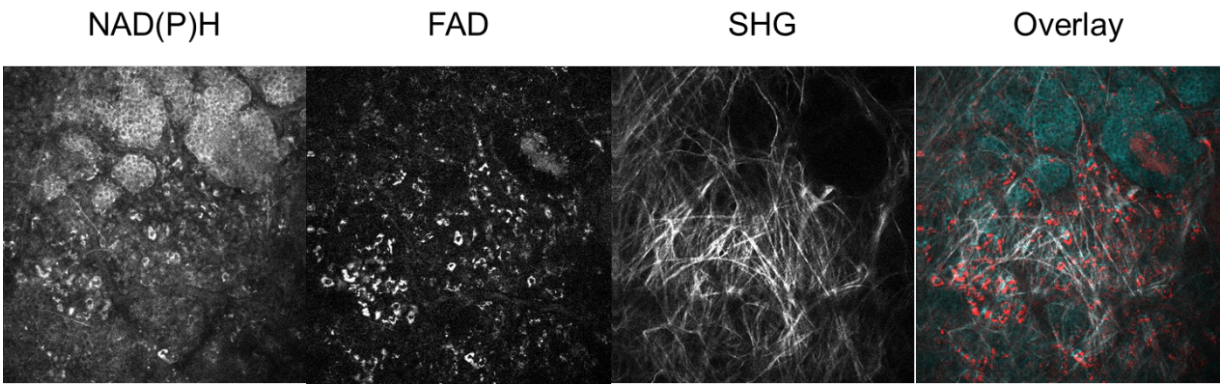

Figure 6: Intravital images collected through an MIW demonstrating extreme stability. NAD(P)H was collected with 20x 1.0NA Plan-Apochromat Water WD 1.7 (Zeiss) (1.878760pix/um) and by exciting 780nm and collecting 445/20, FAD excited using 890nm and collected 562/40, SHG generated using 890nm and collected 445/20.

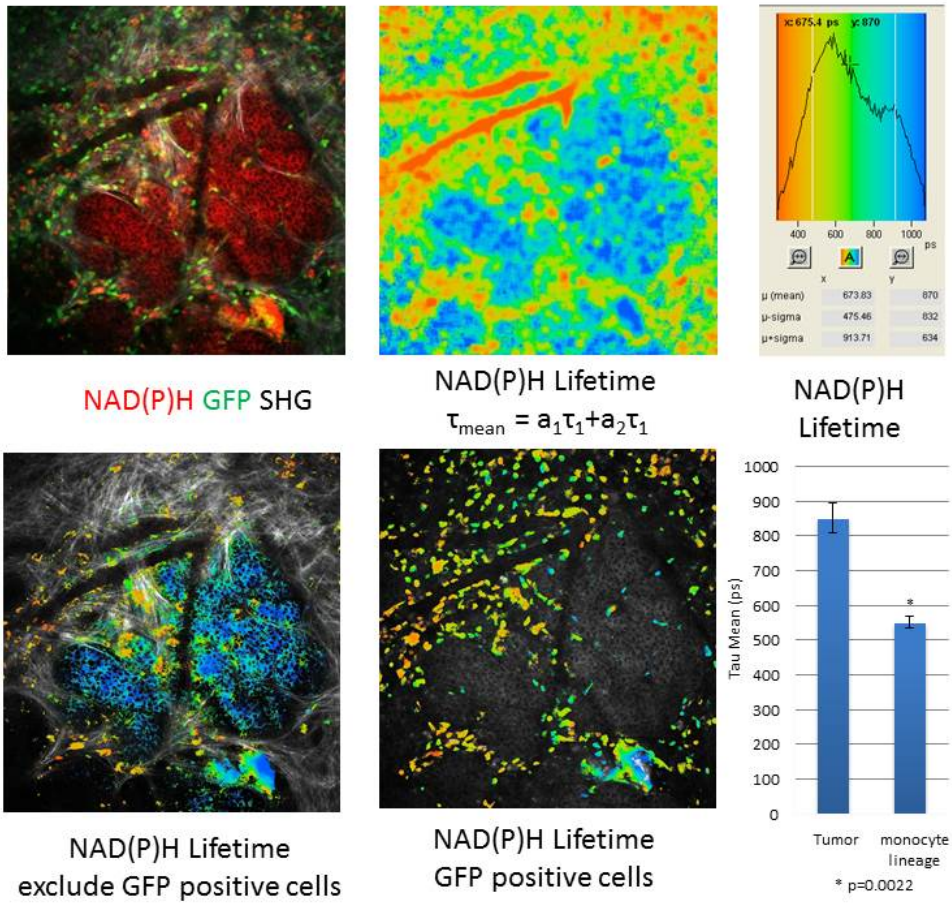

Figure 7: Intravital imaging under mammary imaging window using transgenic mouse expressing c-fms-GFP in monocyte lineage. NAD(P)H was collected with 20x 1.0NA Plan-Apochromat Water WD 1.7 (Zeiss) (1.878760pix/um) and by exciting 780nm and collecting 445/20, GFP excited using 890nm and collected 520/35, SHG generated using 890nm and collected 445/20. FLIM of NAD(P)H with color mapping based on Tau mean from 300ps (red) to 1100ps (blue).

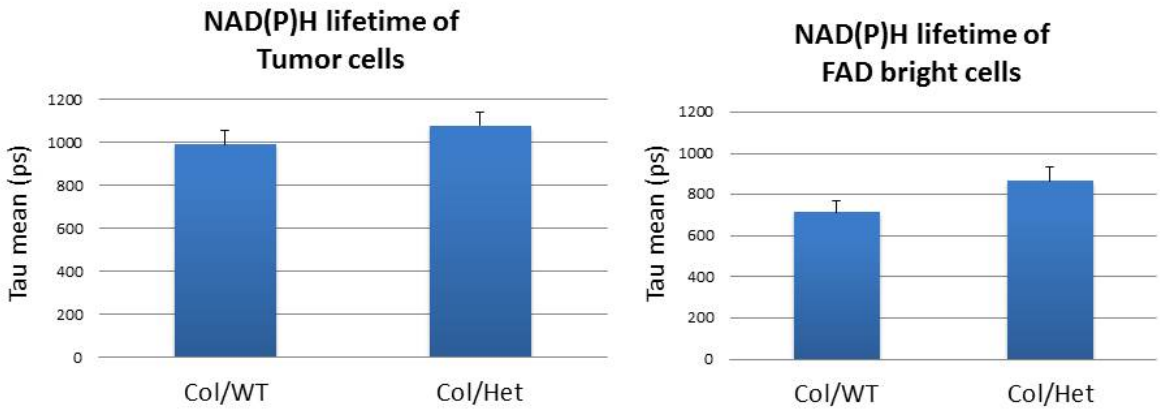

Figure 8: Intravital imaging under mammary imaging window using PyVT/Col1a1-/- mouse and a PyVT/Col1a1+/- mouse. NAD(P)H lifetime was collected with 20x 1.0NA Plan-Apochromat Water WD 1.7 (Zeiss) (1.878760pix/um) and by exciting 780nm and collecting 445/20. Though there was no statistical significance, we need to repeat this experiment to improve statistics.